Available online at www.sciencedirect.com
SCIENCE DIRECT®
Journal of Organometallic Chemistry 680 (2003) 148–154
Journal of Organometallic Chemistry
www.elsevier.com/locate/jorganchem

Density functional theory studies on structural isomers and bonding of catecholborane adducts of Group 5 metallocene (Nb, Ta) hydride complexes

Dan Liu, King-Chung Lam, Zhenyang Lin *

Department of Chemistry and Open Laboratory of Chirotechnology of Institute of Molecular Technology for Drug Discovery and Synthesis, The Hong Kong University of Science and Technology, Clear Water Bay, Kowloon, Hong Kong

Received 22 February 2003; received in revised form 18 April 2003; accepted 18 April 2003

Abstract

Density functional theory calculations at the Becke3LYP level have been performed to study structural isomers of borane adducts of $Cp_2M(H)$ (M = Nb, Ta). Results of calculations show that O- and N-substituted borane adducts can have various structural isomers including boryl, hydridoborate and σ-complex structures. H-, alkyl- and Cl-substituted borane adducts are found to adopt hydridoborate structures. The structural feature is closely related to how the electron-deficient boron center is electronically saturated.

Keywords: Group 5 metallocene (Nb, Ta) hydride HBcat adducts; Structural isomers; Density functional theory calculations

1. Introduction

Of considerable interests are synthetic and structural studies of Groups 4 and 5 metallocene boron-containing complexes [1–20]. Various compounds which can be classified as borane σ-complexes, hydridoborates and boryl complexes have been experimentally reported to date. Results of detailed examinations for these reported complexes suggest that their structures and bonding depend greatly on electronic properties of the metal center, molecular environment as well as substituents on the boron atom. For example, the strongly electrophillic $HB(C_6F_5)_2$ [13,14], BH_3 [6,19,20], and HBR_2 [15–18] (e.g. 9-borabicyclononane) substrates are unexceptionally found to form hydridoborate complexes with metal hydride fragments (see **A**), in which the 'hungry' electron-deficient B atom is electronically satisfied. Those alkoxy-substituted borane substrates [2–10] (HBcat or the substituted HBcat′) with electron pairs on O partially delocalized to the vacant p-orbital on B can serve as a part of a hydridoborate ligand or a η^2-HBcat one, such as the one in $Cp_2Ti(L)(\eta^2$-HBcat) (see **B**) [10,11,20]. Another type of η^2-HBcat complexes (see **C**) contains weak interaction between the B center and its adjacent ligand due to the boron's electron-deficient properties [4,5,10,20]. Clearly, metal centers and molecular environment play key roles to the resulting structural isomers of the alkoxy-substituted borane complexes.

Complicated structural isomers have been reported for HBcat adducts of $Cp_2Nb(H)$ on the basis of ^{1}H-, ^{2}H- and ^{11}B-NMR and X-ray structural studies (see **D**) [2,7,9]. The isomers include the borane σ-complex exo-$Cp_2Nb(H)(\eta^2$-HBcat), hydridoborate $Cp_2Nb(\mu$-$H)_2$(Bcat) and dihydride boryl $Cp_2Nb(H)_2$(Bcat) complexes. Interestingly, the latter two structures were found to be rapidly equilibrating, which was probed by an NMR isotopic perturbation of equilibrium [2]. However, the HBcat adduct of the same group

* Corresponding author. Tel.: +852-23-58-7379.

0022-328X/03/$ - see front matter
doi:10.1016/S0022-328X(03)00311-5

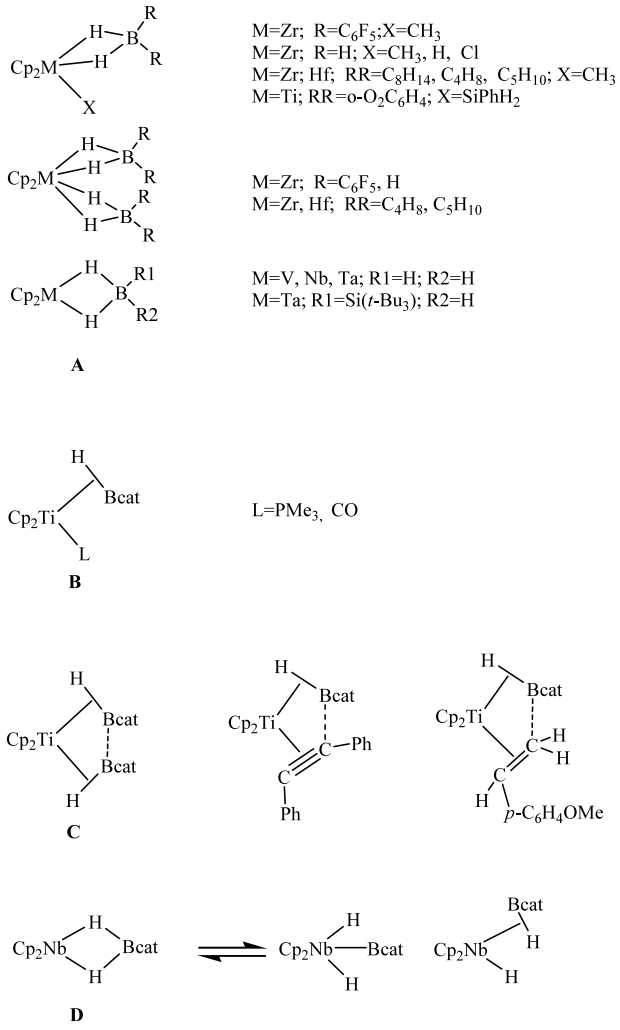

$Cp_2Ta(H)$ fragment was unexpectedly shown to exclusively adopt the endo- and exo-dihydride boryl isomers $Cp_2Ta(H)_2(Bcat)$, different from the isomers of the HBcat adducts of $Cp_2Nb(H)$ [3].

Because of the difference in the structural isomerism between the HBcat adducts of the Nb and Ta metallocene complexes, different mechanisms have been proposed for the Nb and Ta metallocene-mediated hydroborations of olefin [9]. Although NMR and X-ray studies have been carried out [2,3,7,9], due to the known limitations of these used experimental techniques, better understanding of their complicated structural isomers and bonding usually requires an aid of quantum chemical calculations. Experimentalists figured out rapid equilibrium between the two limiting isomers of $Cp_2Nb(\mu\text{-}H)_2(Bcat)$ and $Cp_2Nb(H)_2(Bcat)$, and observed that ^{1}H-NMR signals can also be assigned to an exo-$Cp_2Nb(H)(\eta^2\text{-}HBcat)$ isomer. However, question is raised that how about the possibility of an endo-$Cp_2Nb(H)(\eta^2\text{-}HBcat)$ isomer [2]. Is it a possible minimum point? How about the stabilities of the two rapidly equilibrating isomers? Related to the rapid equilibrium, can a transition state between them be located in such a limited wedge? If located, what is the barrier?

To answer these questions, the density functional method at the Becke3LYP (B3LYP) level was employed to study the structural isomers of the HBcat adducts of Group 5 metallocene hydride fragments. In this paper, calculations are also carried out for substituted borane adducts of the niobocene and tantalocene hydride fragments to study the substituent influences on the structural isomers. The substituents chosen range from H, alkyl, amino to chloride. We hope that these studies provide a better understanding of structures and bonding in this important class of transition metal complexes.

2. Computational details

On the basis of the fact that the B3LYP method [21] can well describe properties of transition metal compounds, all the geometries have been optimized using this method. The effective core potentials of Hay and Wadt with a double-ζ valence basis set (LanL2DZ) are used to describe the Nb and Ta atoms, whereas the 6-31G basis set [22] is used for all other atoms. Polarization functions are added for B ($\zeta(d) = 0.388$) and for those H atoms ($\zeta(p) = 1.1$) directly bonded to the transition metal center. For computational simplicity, HBcat is modeled by $HB(OC_2H_2O)$. Frequency calculations were performed for all calculated structures to confirm their characteristics as minima or transition states. All calculations were performed using the GAUSSIAN-98 software package [23].

3. Results and discussion

The HBcat adducts of $Cp_2M(H)$ (M = Nb, Ta) can be cleanly obtained from the metal-mediated hydroboration reactions of $Cp_2M(H)(\eta^2\text{-}CH_2{=}CH_2)$ in room temperature [7,9]. Earlier, the HBcat adducts of $Cp_2Nb(H)$ and $Cp_2Ta(H)$ were synthesized through mixture of $Cp_2Nb(H)_3$ and $Cp_2Ta(H)_2Li$ with HBcat and ClBcat, respectively [2,3]. Here we focus on the structural isomers and bonding studies of the HBcat adducts of $Cp_2M(H)$ and the substituent effects using the density functional theory (DFT) method described in Section 2.

3.1. Isomers of the $Cp_2Nb(H) + HB(OC_2H_2O)$ adduct

Fully optimized isomers of the $Cp_2Nb(H) + HB(OC_2H_2O)$ adduct are shown in Fig. 1a. Three structural isomers were located. The hydridoborate isomer (**1**) contains a typical interaction between the Cp_2Nb

fragment and a hydridoborate ligand $[H_2Bcat]^-$. Both the endo- and exo-isomers (**2** and **3**) are borane σ-complexes containing an η^2-borane ligand, which is different from the oxidatively-added boryl hydride complex suggested by the X-ray structure [2]. The H2–B bond distances in the σ-complex endo- and exo-isomers (**2** and **3**) were calculated to be 1.491 and 1.391 Å, respectively. The large charge concentrations between the B and H2 atoms have been found in the corresponding Laplacian electron density plots obtained from the B3LYP calculations (Fig. 1b), indicating a σ-complex structural character. In the Laplacian plots, solid contour lines denote $\nabla^2\rho < 0$, where the electron density is locally concentrated; dashed contour lines denote $\nabla^2\rho > 0$, where the electron density is locally depleted.

The hydridoborate isomer (**1**) and the two σ-complex isomers (**2** and **3**, endo- and exo-isomers) were calculated to have roughly equal stability at the B3LYP level (Fig. 1a). The transition state connecting the endo-isomer and hydridoborate isomer was also located. The optimized transition structure (**4**) and barrier are also shown in Fig. 1a. The barrier was calculated to be only 1.0 kcal mol^{-1}. The structural feature of the isomers and their roughly equal stability indicate that the $Cp_2Nb(H)+HB(OC_2H_2O)$ adduct favors structures having a low oxidation state with a formal d^2 electron configuration for the metal center.

The rich structural isomers of the $Cp_2Nb(H)+HB(OC_2H_2O)$ adduct can provide good understanding to the experimental observations [2,7]. The X-ray structure of $Cp_2Nb(H_2Bcat)$ [2] gives the Nb–B distance at 2.292 Å and the H–Nb–H angle at 92.2°. In $Cp_2{}_*Nb(H_2Bcat')$ (Bcat′ = B-1,2-$O_2C_6H_3$-3-^{t}Bu) [7], the Nb–B bond distance is 2.348 Å and the H–Nb–H angle is 72.6°. These two complexes can be considered as representatives of the hydridoborate $[Cp_2{}_*Nb(H_2Bcat')]$ and the endo-isomer $[Cp_2Nb(H)(\eta^2\text{-HBcat}')]$ structures presented in Fig. 1a. The stronger donating Cp* ligand in comparison to Cp weakens the ligand coordinating ability of the $Cp_2{}_*Nb$ fragment, giving a traditional hydridoborate structure. The exo-isomer structure can be found in the tantalum analogue, exo-$Cp_2Ta(H)(\eta^2$-HBcat) [9]. The exo-$Cp_2Nb(H)(\eta^2$-HBcat) can be expected to exist based on its high stability from our calculations (Fig. 1a).

A rapid equilibrium between the hydridoborate isomer and the endo-isomer can be expected to occur because of the roughly equal stability of the two isomers and the very low barrier connecting them (Scheme 1). The stability of both the endo- and exo-isomers of $Cp_2Nb(H)(\eta^2$-HBcat) and the rapid isomerization between the hydridoborate and endo-isomer structures can be used to explain the extensive H/D scrambling phenomena between the hydride ligand of $Cp_2Nb(H)(\eta^2$-olefin) and DBcat observed in the olefin hydroboration reactions [2,9].

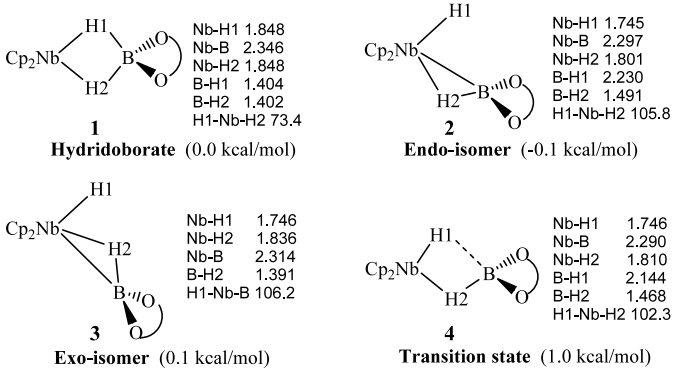

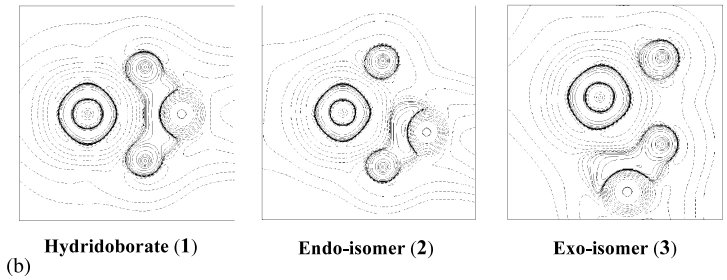

Fig. 1. (a) Calculated structures and relative energies of the structural isomers of the $Cp_2Nb(H)+HB(OC_2H_2O)$ adduct and the transition state connecting the hydridoborate and endo-isomer. (b) The corresponding Laplacian electron density plots for the hydridoborate, endo- and exo-isomers on the plane containing the H1, Nb, H2 and B atoms.

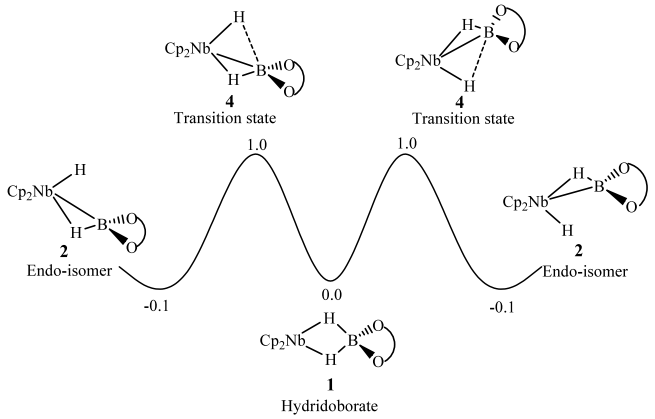

Scheme 1.

3.2. Isomers of the $Cp_2Ta(H)+HB(OC_2H_2O)$ adduct

Isomers of the $Cp_2Ta(H)+HB(OC_2H_2O)$ adduct have been optimized. Two fully optimized structures are shown in Fig. 2a. Interestingly, there is no corresponding η^2-HBcat endo-isomer for the tantalocene hydride adduct. Instead, a boryl structure (**5**) with a formal d^0 metal center was located. In the boryl structure, the B–H1 and B–H2 distances are calculated to be 2.085 and 2.086 Å, respectively, indicating no interactions between the H and B atoms. The Ta–B distance is calculated to be 2.293 Å, in a good agreement with 2.263 Å from the X-ray crystal structure [2]. The H1–Ta–H2 bond angle is as large as 120.7°, much larger than those of σ-complex structures (**2** and **3**) discussed above for the niobium adduct ($<107.0°$). A hydridoborate structure (Ta analog of **1**) was also obtained from our geometry optimizations. However, the energy of this hydridoborate structure is lying 5.5 kcal mol^{-1} higher than that of the boryl structure. In addition, the structure is found to be very close to the transition structure connecting itself and the boryl structure. Furthermore, the energy is almost equal to that of the transition structure. These calculation results suggest that the hydridoborate structure might not be a true stationary point. Indeed, $Cp_2Ta(H)_2(Bcat)$ is believed to be a boryl hydride complex. The instability of the hydridoborate structure can be related to the fact that the B–O π bonding interactions are very strong.

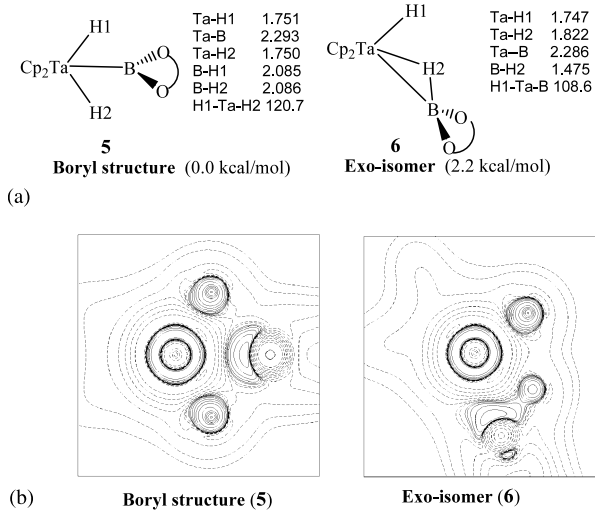

Fig. 2. (a) Calculated structures and relative energies of the structural isomers of the $Cp_2Ta(H)+HB(OC_2H_2O)$ adduct. (b) The corresponding plots of Laplacian electron density on the plane containing the H1, Ta, H2 and B atoms.

The exo-isomer (**6**) of the adduct adopts a σ-complex structure $Cp_2Ta(H)(\eta^2\text{-}HB(OC_2H_2O))$, rather than a boryl structure having a formal oxidation state of +5 for the metal center. The B–H2 and Ta–B distances are calculated to be 1.475 and 2.286 Å, very close to the distances of 1.450 and 2.295 Å, respectively, reported in the X-ray crystal structure [3]. Although Ta tends to have a high oxidation state with a formal d^0 electron configuration, the steric repulsion between the $HB(OC_2H_2O)$ group and the two Cp rings may prevent an expansion of ligand spread angle in the wedge, promoting the formation of an η^2-$HB(OC_2H_2O)$ structure. Thus, the exo-$Cp_2Ta(H)(\eta^2\text{-}HB(OC_2H_2O))$ σ-complex structure (**6**) is formed as a result of a compromise between the electronic interactions and steric repulsions. In energy, the exo-isomer (**6**) is 2.2 kcal mol^{-1} less stable than the boryl structure (**5**).

The Laplacian electron density plots, shown in Fig. 2b, provide further support to the structural classification mentioned above. The boryl structure does not have a B–H interaction while the exo-isomer has significant charge concentrations along the B–H bond.

Different from the niobocene analogue featured with a rapid equilibrium between structural isomers [2,9], which allows extensive deuterium incorporations in the presence of DBcat, the resulting structural preference of the tantalocene analogue implies that the deuterium incorporation in the HBcat adduct of $Cp_2Ta(H)$ is not as easy as that in the niobocene analogue, well consistent with experimental observations [9].

3.3. Isomers of the $Cp_2MB(OC_2H_2O)$ (M = Nb, Ta) + $HB(OC_2H_2O)$ adducts

The structural isomers of $Cp_2M(Bcat)$ (M = Nb, Ta)+HBcat adducts have also been investigated. Experimentally, the $Cp_2Nb(Bcat)$+HBcat adduct was obtained in the study of an olefin hydroboration mediated by the $Cp_2Nb(H)$ fragment [9]. Interestingly, the X-ray structure of the niobium adduct shows a crystallographic equivalence of the two Bcat ligands, which were not anticipated because the ^{1}H- and ^{11}B-NMR spectra indicate chemically distinct Bcat units. Due to the limitation of the X-ray technique for location of hydrogen atoms, a boryl hydride $Cp_2Nb(H)(Bcat)_2$, in which the two Bcat ligands are next to each other and

the hydride occupies one of the two exo positions in the metallocene wedge, was proposed. A borane σ-complex structure was not suggested because borane elimination chemistry (substitution reactions) was not observed. On the contrary, our calculations for the $Cp_2Nb(B(OC_2H_2O))+HB(OC_2H_2O)$ adduct give two borane σ-complex structural isomers (**7** and **8**) (Fig. 3a). The lowest energy isomer indeed has the hydride in one of the two exo positions. The inconsistence between our calculated structures and the proposed one suggests that there might be other factors affecting the borane substitution reaction by a carbonyl ligand used in the experiment [7]. The substitution product $Cp_2Nb(Bcat)(CO)$ may not be very stable because both Bcat and CO compete for backbonding interaction with the metal center. The Laplacian electron density plot of the lowest energy isomer shows a noticeable interaction between the two boron centers (Fig. 3b). The additional interaction may also affect the substitution reaction.

The calculated isomers of the $Cp_2Ta(B(OC_2H_2O))+HB(OC_2H_2O)$ adduct adopt borane σ-complex structures (**9** and **10**), similar to the situation found for the niobium adduct. The exo-isomer (**9**) is found to be more stable (Fig. 3c).

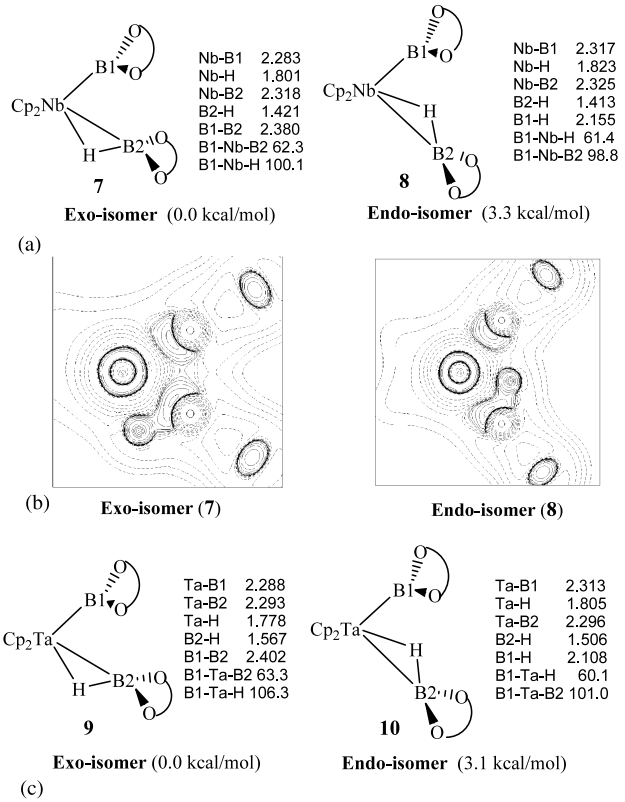

Fig. 3. (a) Calculated structures and relative energies of the structural isomers of the $Cp_2Nb(B(OC_2H_2O))+HB(OC_2H_2O)$ adduct. (b) The corresponding plots of Laplacian electron density on the plane containing the B1, Nb, H and B2 atoms. (c) Calculated structures and relative energies of the structural isomers of the $Cp_2Ta(B(OC_2H_2O))+HB(OC_2H_2O)$ adduct.

3.4. Substitutent effects on structural isomers of borane adducts of $Cp_2M(H)$ ($M = Nb, Ta$)

Substituents on B have been found to have significant effects on structures of various borane adducts described in Section 1. Substituents, ranging from H, Me and NH_2 to Cl, were used to study the structures of $Cp_2M(H)$ ($M = Nb, Ta$) + HBR_2 adducts. As expected, the H- and Me-substituted borane adducts of $Cp_2M(H)$ ($M = Nb, Ta$) exclusively adopt a hydridoborate structure (**11**) (Fig. 4a), where the 'very hungry' electron-deficient B center can be electronically satisfied. In all the calculations, neither boryl structures nor endo η^2-HBR_2 σ-complex structures can be located. The η^2-HBR_2 exo-isomers, in each of which the BR_2 unit occupies one position and cannot interact with the hydride in the other exo position, can be located. However, their energies are much higher by ca. 5.0–9.0 kcal mol^{-1} than their corresponding hydridoborate structural isomers.

NH_2-substituted borane adducts of $Cp_2M(H)$ ($M =$ Nb, Ta), in which the NH_2 substituents allow the electron pairs on N partially delocalized to the vacant p orbital on B, have structural isomers analogous to the adducts having OC_2H_2O substituents. For the Nb species, hydridoborate (**13**), η^2-$HB(NH_2)_2$ endo- and exo-isomers (**12** and **14**) have been located (Fig. 4b). In both the endo- and exo-isomers, the Nb···B distances are found to be remarkably long. Apparently, the extremely strong B–N π bonding interaction is responsible for the long Nb···B distances. In the calculated structures (**12** and **14**), a roughly planar geometry can be found around each of the N centers, providing evidence of the extreme strong B–N π bonding interactions. In addition, the two NH_2 structural moieties and the B–H2 bond in each of the two structures (**12** and **14**) are almost coplanar, indicating that the B–N π bonding interactions are very strong, which prevent the boron center from further bonding with the metal center and give the remarkably long Nb···B distances. For the Ta species, boryl (**15**) and η^2-$HB(NH_2)_2$ exo-isomer (**16**) structures were located (Fig. 4c). Again, the η^2-$HB(NH_2)_2$ exo-isomer (**16**) structure, similar to structure **14**, has a very long Ta···B distance. The boryl structure has higher stability, lying 3.4 kcal mol^{-1} lower than the exo-isomer. The Cl-substituted borane adducts of $Cp_2M(H)$ ($M = Nb, Ta$) were also calculated. They adopt hydridoborate isomers (**11**). Apparently the π-donating ability of chloride is not strong enough to stabilize a boryl structure or a η^2-$HBCl_2$ endo-isomer.

4. Conclusion

The calculation results show that the O- and N-substituted borane adducts of $Cp_2M(H)$ ($M = Nb, Ta$)

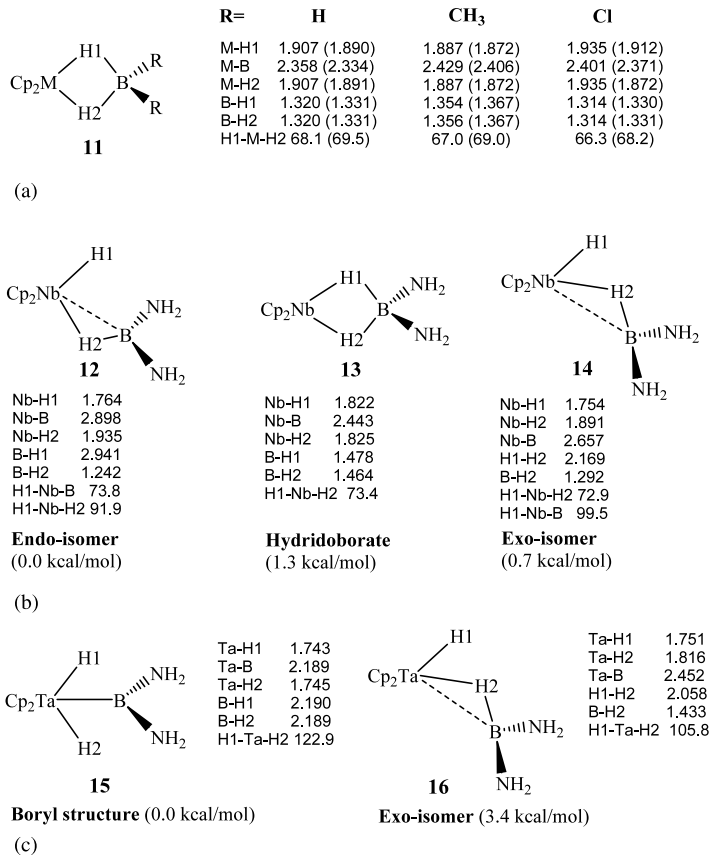

Fig. 4. (a) Optimized H-, CH_3- and Cl-substituted hydridoborate structures of the Nb and Ta metallocenes. Structural parameters of the Ta metallocenes are shown in parenthesis. (b) Calculated structures and relative energies of the structural isomers of the $Cp_2Nb(H)+HB(NH_2)_2$ adduct. (c) Calculated structures and relative energies of the structural isomers of the $Cp_2Ta(H)+HB(NH_2)_2$ adduct.

have various structural isomers including hydridoborate, σ-complex endo- and exo-isomer structures containing η^2-HB coordination. The simultaneous existence of hydridoborate (**1**) and endo-isomer (**2**) structures as local minima in the potential energy surface is unique because the two structures differ mainly in one of the B $\cdots$H contacts. This feature is closely related to the delicate bonding balance within the NbH_2B structural unit. For adducts of $Cp_2Ta(H)$, boryl structures and σ-complex exo-isomers are located. Boryl structures, instead of hydridoborate ones, become the local minima, reflecting the periodic property that Ta prefers a higher formal oxidation state in comparison to Nb. For H-, alkyl- and Cl-substituted borane adducts, hydridoborate structures (**11**) are the most favorable because the electron-deficient boron center in other type of structural arrangements cannot be effectively saturated.

Acknowledgements

This work was supported by the Research Grants Council of Hong Kong and the University Grants Committee of Hong Kong through the Area of Excellence Scheme (Aoe).

References

[1] Q. Jiang, P.J. Carroll, D.H. Berry, Organometallics 12 (1993) 177.
[2] J.F. Hartwig, S.R. De Gala, J. Am. Chem. Soc. 116 (1994) 3661.
[3] D.R. Lantero, D.H. Motry, D.L. Ward, M.R. Smith, III, J Am. Chem. Soc. 116 (1994) 10811.
[4] X.M. He, J.F. Hartwig, J. Am. Chem. Soc. 118 (1996) 1696.
[5] J.F. Hartwig, N. Muhoro, X.M. He, O. Eisenstein, R. Bosque, F. Maseras, J. Am. Chem. Soc. 118 (1996) 10936.
[6] S. Camanyes, F. Maseras, M. Moreno, A. Lledós, J.M. Lluch, J. Bertrán, Angew. Chem. Int. Ed. Engl. 36 (1997) 265.
[7] D.R. Lantero, D.L. Ward, M.R. Smith, III, J. Am. Chem. Soc. 119 (1997) 9699.
[8] N. Muhoro, J.F. Hartwig, Angew. Chem. Int. Ed. Engl. 36 (1997) 1510.
[9] D.R. Lantero, S.L. Miller, J.Y. Cho, D.L. Ward, M.R. Smith, III, Organometallics 18 (1999) 235.
[10] N. Muhoro, X.M. He, J.F. Hartwig, J. Am. Chem. Soc. 121 (1999) 5033.
[11] W.H. Lam, Z. Lin, Organometallics 19 (2000) 2625.
[12] A. Antiñolo, F. Carrillo-Hermosilla, J. Fernández-Baeza, S. García-Yuste, A. Otero, A.M. Rodríguez, J. Sánchez-Prada, E. Villaseñor, R. Gelabert, M. Moreno, J.M. Lluch, A. Lledós, Organometallics 19 (2000) 3654.
[13] Y.M. Sun, W.E. Pies, S.J. Rettig, Organometallics 15 (1996) 4110.

[14] R. Choukroun, B. Douziech, B. Donnadieu, Organometallics 16 (1997) 5517.
[15] R.E.V.H. Spence, W.E. Piers, Y.M. Sun, M. Parvez, L.R. MacGillivray, M.J. Zaworotko, Organometallics 17 (1998) 2459.
[16] G.T. Jordan, IV, F. Liu, S.G. Shore, Inorg. Chem. 36 (1997) 5597.
[17] J. Liu, E.A. Meyers, S.G. Shore, Inorg. Chem. 37 (1998) 496.
[18] F. Liu, J.P. Liu, E.A. Meyers, S.G. Shore, Inorg. Chem. 37 (1998) 3293.
[19] S.L.J. Conway, L.H. Doerrer, M.L.H. Green, M.A. Leech, Organometallics 19 (2000) 630.
[20] D. Liu, K.-C. Lam, Z. Lin, Organometallics, in press.
[21] (a) A.D. Becke, J. Chem. Phys. 98 (1993) 5648;
(b) B. Miehlich, A. Savin, H. Preuss, Chem. Phys. Lett. 157 (1989) 200;
(c) C. Lee, W.T. Yang, G. Parr, Phys. Rev. B 37 (1988) 785.
[22] (a) M.S. Gordon, Chem. Phys. Lett. 76 (1980) 163;
(b) P.C. Hariharan, J.A. Pople, Theor. Chim. Acta 28 (1973) 213;
(c) R.C. Binning, Jr., L.A. Curtiss, J. Comput. Chem. 11 (1990) 1206.
[23] M.J. Frisch, G.W. Trucks, H.B. Schlegel, G.E. Scuseria, M.A. Robb, J.R. Cheeseman, V.G. Zakrzewski, J.A. Montgomery, Jr., R.E. Stratmann, J.C. Burant, S. Dapprich, J.M. Millam, A.D. Daniels, K.N. Kudin, M.C. Strain, O. Farkas, J. Tomasi, V. Barone, M. Cossi, R. Cammi, B. Mennucci, C. Pomelli, C. Adamo, S. Clifford, J. Ochterski, G.A. Petersson, P.Y. Ayala, Q. Cui, K. Morokuma, D.K. Malick, A.D. Rabuck, K. Raghavachari, J.B. Foresman, J. Cioslowski, J.V. Ortiz, B.B. Stefanov, G. Liu, A. Liashenko, P. Piskorz, I. Komaromi, R. Gomperts, R.L. Martin, D.J. Fox, T. Keith, M.A. Al-Laham, C.Y. Peng, A. Nanayakkara, C. Gonzalez, M. Challacombe, P.M.W. Gill, B. Johnson, W. Chen, M.W. Wong, J.L. Andres, C. Gonzalez, M. Head-Gordon, E.S. Replogle, J.A. Pople, GAUSSIAN-98 (Revision A.9), Gaussian, Inc, Pittsburgh, PA, 1998.